Toxicologic Pathology, 33:386–397, 2005

ISSN: 0192-6233 print / 1533-1601 online
DOI: 10.1080/01926230590930272

An Investigation of the Effects of Late-Onset Dietary Restriction on Prostate Cancer Development in the TRAMP Mouse

ANDREW W. SUTTIE,[1] GREGG E. DINSE,[2] ABRAHAM NYSKA,[3] GLENDA J. MOSER,[1] THOMAS L. GOLDSWORTHY,[1] AND ROBERT R. MARONPOT[3]

[1]*Integrated Laboratory Systems, Research Triangle Park, North Carolina 27709, USA*
[2]*Biostatistics Branch,*[3]*Laboratory of Experimental Pathology, National Institute of Environmental Health Sciences (NIEHS), Research Triangle Park, North Carolina 27709, USA*

ABSTRACT

In our previous work we showed that dietary restriction initiated at puberty reduced prostate cancer development in the TRAMP mouse model. The current study was conducted to ascertain whether a dietary restriction regime would similarly reduce lesion development if imposed once tumor development was well established. Male TRAMP mice were maintained on an ad libitum diet until 20 weeks of age when proliferative prostate lesions are clearly evident. Mice were then subjected to a 20% restriction in dietary calories compared to matched controls, which were continued on ad libitum feeding. Mice were sacrificed at 20, 24, 32, and 39 weeks of age and proliferative epithelial lesions of the prostate were assessed using an established grading scheme. In this study, although dietary restriction reduced mean sex pluck weight (prostate and seminal vesicles), and mean grade of epithelial proliferative lesions in the dorsal and lateral lobes of the prostate, the effect was not as pronounced as was the case with dietary restriction from puberty. There was no relationship between serum insulin like growth factor (IGF-1) and prostate lesion grade. Additionally, we also report the relationship between lobe specific lesion development and SV40 immunostaining and, the occurance of neuroendocrine tumors (NETs) in the ventral prostate and urethra of the TRAMP mouse. NETs stained with high specificity and sensitivity for the neuroendocrine markers, synaptophysin and neuron-specific enolase (NSE), less for serotonin, but not for chromogranin A. NETs did not stain for cyclo-oxygenase-2 (COX-2) nor androgen receptor (AR). SV40 positive tubulo-acinar tumors seen occasionally in the kidney, did not stain for synaptophysin nor NSE.

Keywords. Diet-restriction; prostate cancer; TRAMP; neuroendocrine.

INTRODUCTION

Prostate cancer is the second most common cause of cancer deaths in men in the United States of America (Jemal et al., 2002). A link between diet and prostate cancer is supported by epidemiological data showing an increased risk of prostate cancer in men moving from low incidence countries to the United States (Giovannucci, 1995). This increased risk may be due to lesser amounts of some dietary components (e.g., soy and isoflavones) in the American diet (Lee et al., 2003) or to increased caloric intake, particularly from fat (Denmark-Wahnefried et al., 2001). The insulin-like growth factor (IGF) axis may play a role in the effects of diet, and also of exercise, in reducing risk of prostate cancer, since prostate cancer is associated with high levels of serum IGF-1. Low-fat diets and exercise decrease serum IGF-1 (Ngo et al., 2003).

The TRAMP (Transgenic Adenocarcinoma of Mouse Prostate) model of prostate cancer developed by Greenberg et al. (1995), is a transgenic line of C57BL/6 mice utilizing a construct comprised of the minimal −426/+28 rat probasin promoter to drive prostate-specific epithelial expression of the SV40 large T antigen (Foster et al., 1997). Probasin is an androgen- and zinc-regulated protein found in the dorsolateral prostate of the rat. Probasin is developmentally regulated and increases in the dorsolateral prostate at sexual maturity, but decreases in the ventral prostate (Greenberg et al., 1994). The TRAMP mouse develops spontaneous, autochthonous prostate cancer, which closely resembles the human disease (Gingrich et al., 1994) with metastasis to regional lymph nodes, lungs, kidney, adrenal, and bone.

The TRAMP mouse has been used in chemopreventative studies; green tea polyphenols, spinach extract, flutamide (an anti-androgen), and R-flurbiprofen (an anti-inflammatory drug) have been shown to inhibit prostate cancer progression in this model (Raghow et al., 2000; Wechter et al., 2000; Gupta et al., 2001; Nyska et al., 2003).

In laboratory rats and mice, a regimen of caloric restriction has been shown to increase survival time and decrease the lifetime incidence of cancers (Pugh et al., 1999; Hubert et al., 2000). We have previously shown that in the TRAMP mouse, dietary restriction when introduced at puberty reduces the rate of progression of proliferative prostate lesions (Suttie et al., 2003). Reduced serum IGF-1 levels have been shown to be associated with attenuation of prostatic cancer progression in the TRAMP mouse (Nyska et al., 2002).

The objective of this work was to establish whether late-onset dietary restriction, initiated when the disease was well established, would have a positive effect in ameliorating lesion development, and whether effects on prostatic lesions were associated with alterations in serum IGF-1. Lesion development was assessed by evaluating the lesion grade in each lobe of the prostate using an established grading scheme (Suttie et al., 2003). These findings would help determine the potential value of late onset dietary restriction in therapeutic strategies for prostate cancer. We selected 20 weeks of age

Address correspondence to: Dr. Andrew Suttie, Integrated Laboratory Systems, Inc., P.O. Box 13501, Research Triangle Park, North Carolina 27709, USA; e-mail: asuttie@ils-inc.com

for the onset of dietary restriction since lesion development is well advanced by this time. Sacrifices were scheduled between 20 weeks and 39 weeks, the life expectancy of this mouse model. Additionally, this work documents lobe specific nature of proliferative epithelial lesion development in the prostate.

Neuroendocrine tumors that were seen in occasional mice from previous studies with earlier sacrifice timepoints were a significant cause of mortality in the present study. In addition to the importance of NETs in limiting the lifespan of our TRAMP mice, they are a malignant tumor type in humans (Bostwick et al., 2002). Therefore, in order to document the immunophenotype for comparison with their counterparts both in humans and in mouse models we stained representative NETs with a panel of neuroendocrine specific antibodies. Also, a hitherto unreported tumor was observed in the kidneys of occasional mice that we also stained to establish whether it was of neuroendocrine origin.

Materials and Methods

Animals and Diet Restriction

Seven groups of homozygous TRAMP male mice established on a C57BL/6 background were housed in an AAALAC-accredited Specific Pathogen-Free (SPF) facility and handled according to the guidelines provided in the NIH *Guide for the Care and Use of Laboratory Animals*. Mice were fed NTP 2000 diet (Zeigler Bros., Gardners, PA). At 20 weeks of age, 109 mice were allocated to either an ad libitum or dietary-restriction feeding regimen (80% of feed consumed by ad libitum group. Measurements of ad libitum consumption and adjustments to diet restricted feed were made twice weekly). Mice were euthanized by CO_2 asphyxiation and subsequent exsanguination at 4 timepoints: 20 weeks of age (12 mice in the ad-libitum group), 24 weeks of age (11 mice in the ad-libitum group and 12 mice in the diet-restricted group), 32 weeks of age (9 mice in the ad-libitum group and 10 mice in the diet-restricted group), and 39 weeks of age (21 mice in the ad-libitum group and 18 mice in the diet-restricted group). Prior to each scheduled necropsy, blood was collected from the retro-orbital sinus and serum was harvested for serum IGF-1 analysis.

A complete necropsy was performed that included examination and removal of all organs. The accessory sex pluck [prostate, seminal vesicles, and anterior prostate (coagulating gland), and urinary bladder] were removed, the urinary bladder was removed, the glands weighed as a whole, and arranged on moistened filter paper in a cassette to prevent curling during fixation and to maintain anatomical relationships. Any abnormal tissues noted at necropsy were also collected. Tissues were emersion fixed in 10% neutral-buffered formalin for 18–24 hours, stored in 70% ethanol, and the prostate prepared for histiologic sectioning according to the methods of Suwa et al. (2002). Five- to 6-μm sections were taken at 200-micron intervals until the embedded tissue was exhausted. All slides were stained with hematoxylin and eosin (H&E) for light microscopic examination. Slides were also evaluated from gross abnormalities noted during necropsy.

Histopathological Evaluation of Prostate

Proliferative lesions of the prostate, including those from animals that died or were sacrificed for humane reasons prior to scheduled sacrifice, were graded according to a scheme established in an earlier dietary restriction study (Suttie et al., 2003).

The most advanced epithelial lesion was identified for each prostate lobe. Lesion severity was graded on a scale of 1 to 6 and the distribution of each lesion, was classified on an ordinal scale: focal (1–2 isolated lesions), multifocal (3 or more isolated lesions up to approximately 30% of the gland involved at the particular grade), or diffuse (in excess of 30% of the gland involved). These scales were combined to give a "distribution-adjusted" lesion grade. Within a grade, a multifocal lesion was considered more severe than a focal lesion but less severe than a diffuse lesion. Further, a focal lesion of a particular grade (e.g., grade 4 focal) was regarded as more severe than a diffuse lesion of a lower grade (e.g., grade 3 diffuse). The distribution-adjusted lesion grade was then obtained by assigning the integers 0 to 18 to each successive rank ordering of these designations (e.g., 0 = normal; 1 = grade 1 focal; 2 = grade 1 multifocal; . . . etc. to 18 = grade 6 diffuse). Neuroendocrine pattern lesions were not included in this evaluation and they are reported separately.

Statistical Evaluation

Standard nonparametric methods (Kaplan and Meier, 1958) were used to estimate survival curves. The endpoint of interest is death from natural causes, with sacrifices yielding censored survival times. Each point on the resulting survival curve provides an estimate of the percentage of mice surviving to a given time.

Multiple regression analysis (Neter et al., 1985) was used to assess whether a particular response was affected by potential explanatory factors. We individually investigated 6 responses: the four lobe-specific lesion grades, IGF concentration, and sex-pluck weight. In each case, we assumed a linear model that expressed the average response as a function of 3 explanatory factors: diet restriction, time on study, and initial body weight. Diet restriction did not start until the mice were 20 weeks of age, so the time on study was taken to be age minus 20 weeks, and initial body weight refers to the weight at 20 weeks of age. Diagnostic plots indicated that the original scale was adequate for all responses except sex-pluck weight, where the reciprocal of the square root led to a better fitting model. The use of a statistical model facilitated the evaluation and summarization of the effects of explanatory factors on each response of interest.

Specifically, our model assumed that each response was a quadratic function of the time on study, which allowed for curvature in the relationship between that response and time. The model included diet by time and diet by time-squared interactions, which permitted diet restriction to modify the way in which the response changed over time. In addition, the model included a main effect for weight, plus weight by diet by time and weight by diet by time-squared interactions, which allowed the average response at 20 weeks of age and the diet effect on the response curve to vary with initial body weight. We purposely did not include a main effect for diet or an interaction between diet and initial weight because there should be no effect of diet restriction at time 0 (i.e., 20 weeks of age). Weight by time and weight by time-squared interactions were not included, and formal statistical tests showed that adding such terms did not significantly enhance

the model. Finally, we applied our analysis only to mice without an NET, which we view as a separate tumor type distinct from the continuum of lesion progression observed with epithelial neoplasms; see the Discussion section for details.

Immunohistochemistry

SV40: Paraffin embedded sections were hydrated through xylene and graded ethanol into 1X automation buffer. Endogenous peroxidases were quenched with 3% hydrogen peroxide for 15 minutes and slides rinsed in 3 changes of automation buffer. Antigen retrieval was performed by steaming in 1X citrate buffer for 30 minutes. Slides were cooled for 20 minutes and rinsed in distilled water. Slides were again rinsed through three changes of automation buffer. Nonspecific binding was blocked by incubation in 10% normal horse serum for 20 minutes. Avidin and biotin blocks were applied for 15 minutes each with a quick rinse in between with automation buffer. Excess blocking solution was removed and primary antibody (mouse anti-SV40 large T antigen; BD Pharmingen, San Diego, CA, catalog no. 554149) applied at 1:100 dilution for 1 hour. Slides were rinsed in two changes of automation buffer for 5 minutes each. Secondary horse anti-mouse IgG biotinylated antibody (1:500) was applied for 30 minutes at room temperature and slides were rinsed again in 2 changes of automation buffer. Visualization was achieved with Vector Standard ABC Elite Kit (Vector Laboratories, Burlingame, CA) label applied for 30 minutes followed by two rinses in automation buffer, treatment with liquid DAB chromogen (Dako) for 6 minutes, then rinsed in tap water and counterstained with modified Harris hematoxylin.

Synaptophysin, Chromagranin A, NSE, Serotonin, COX-2, AR

Paraffin embedded sections were heated at 60°C then hydrated through xylene and graded ethanol. Endogenous peroxidases were quenched in 3% hydrogen peroxide for 8 minutes and slides were rinsed in deionized water. Epitope retrieval was performed by steaming with Target Retrieval Solution (DAB) at 88°C for 20 minutes. Slides were rinsed in deionized water followed by three changes of PBS (Sigma), then 1% BSA/PBS (Jacobson Immuno Research Labs) was added to enhance antibody adherence. Non-specific binding was blocked with CYTO A Background Buster (Innovex Biosciences) for 30 minutes followed by Avidin/Biotin Blocking kit (Vector Lab). Primary antibodies used were Synaptophysin: Rabbit polyclonal, Santa Cruz Biotechnology, Inc. (catalog no. SYP(H-93):sc-9116), Chromogranin A: Rabbit polyclonal, Santa Cruz Biotechnology, Inc. (catalog no. Chr-A(H-300):sc-13090), NSE: Rabbit anti-bovine polyclonal, Biomeda (catalog no. V2004), Serotonin: Rat monoclonal, Abcam (catalog no. YC5/45), AR: Rabbit polyclonal, Upstate (catalog no. 06-680), COX-2: Rabbit polyclonal, Cayman (catalog no. 160106). These were applied at manufacturers' recommended dilutions in 1% BSA/PBS for one hour and slides were rinsed in three changes of PBS. Secondly anti-Rabbit IgG Detection Kit (Vector Labs) was applied for 30 minutes and slides rinsed in three changes of PBS. Visualization was achieved by staining with ABC Elite Complex (anti-Rabbit Detection Kit, Vector Labs) for 30 minutes, followed by rinsing in three changes of PBS then Chromogen (DAB substrate solution, DAKO) for 3 minutes; then rinsing in tap water and counterstaining with modified Harris hematoxylin. Positive controls used were human brain for synaptophysin, Chromogranin A, serotonin and NSE, mouse ureter for COX-2, and mouse testis for AR. Negative controls consisted of test tissues and positive control tissues without primary antibody.

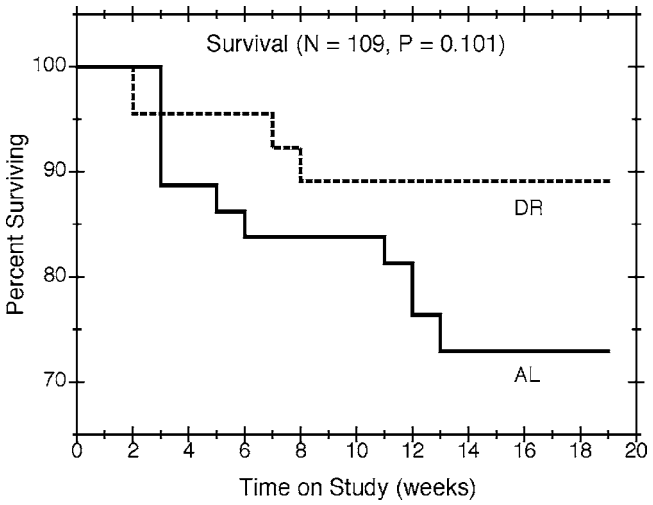

FIGURE 1.—Survival by time on study and feeding group. Nonparametric estimates of the survival percentages are plotted against time for all mice in the study, with solid and dashed lines showing the estimates for the ad libitum (AL) and diet restricted (DR) groups, respectively.

RESULTS

Survival

Estimates of survival percentages are plotted against time on study in Figure 1. The curves suggest that mice in the dietary restriction group lived longer than mice fed ad libitum, but the apparent differences in survival were not statistically significant ($p = 0.101$). Due to the relatively small number of mice dying before scheduled sacrifice, most of the times to death from natural causes were censored, which limits the informativeness of the estimates and the power to detect survival differences.

Lesion Grade

Of the 84 mice that died without an NET, lesions in the anterior, dorsal, lateral, and ventral lobes of the prostate were graded for 84, 84, 81, and 74 mice, respectively. The observed severity grades for individual mice are plotted against time on study in Figure 2. We also plot reference curves, which display the lesion grades that our model would predict at each possible value of time on study for mice with an initial body weight equal to the overall average. The vertical spread of the symbols provides a sense of the variability in the data. For each lobe, lesions tended to get more severe over time. The reference curves in Figure 2 show that the grades expected for mice of an average initial body weight increased with the time on study, except possibly for lesions in the anterior lobe among diet restricted mice. Relative to ad libitum feeding, diet restriction lessened the rate at which lesions became more severe over time in the dorsal ($p = 0.002$) and lateral

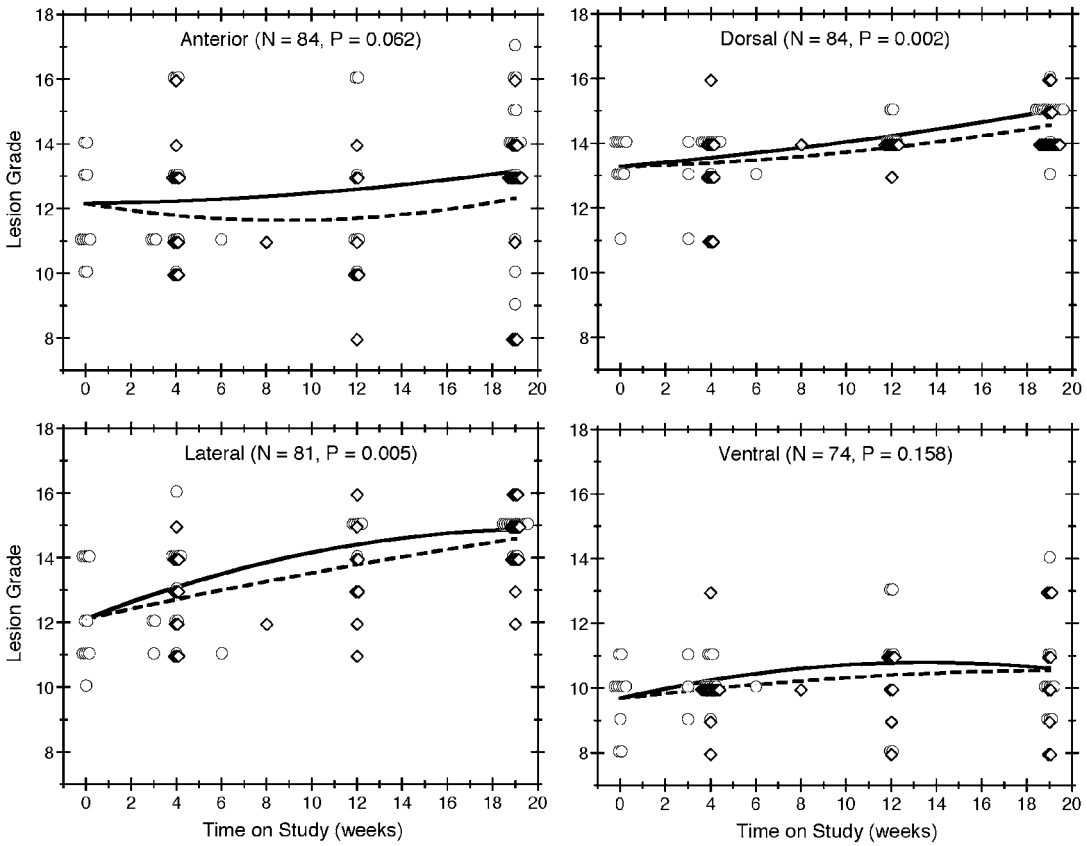

FIGURE 2.—Lesion grade by time-on-study, feeding group, and prostate lobe. Lesion grades are plotted over time for all mice without an NET, with each quadrant of the figure showing the results for a different lobe of the prostate. Observations in the ad libitum group are depicted by circles and observations in the diet restricted group are depicted by diamonds. Multiple mice having the same grade at the same death time are indicated by horizontally staggered symbols. The symbols also are staggered vertically to distinguish the 2 feeding protocols. The solid and dashed lines show the expected grades in the ad libitum and diet restricted groups, respectively, for reference mice (i.e., those with an initial body weight equal to the average).

($p = 0.005$) lobes. Figure 2 suggests similar results in the anterior ($p = 0.062$) and ventral ($p = 0.158$) lobes, but these differences were not statistically significant.

IGF Serum Concentration

Individual IGF serum concentrations were observed for 74 of the mice without an NET and are plotted against time on study in Figure 3, along with reference curves that illustrate the serum concentrations our model would predict for mice of an average initial body weight. Generally, the IGF serum concentrations decreased over time for all mice. Compared to ad libitum feeding, diet restriction appeared to hasten the decrease in IGF serum concentration over time, as depicted by the reference curves in Figure 3, but this effect was not statistically significant ($p = 0.204$).

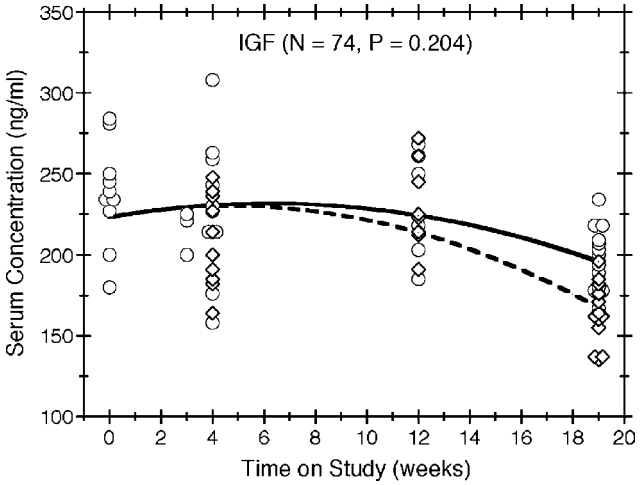

FIGURE 3.—Serum IGF concentration by time on study and feeding group. IGF concentrations are plotted over time for all mice without an NET, with circles and diamonds depicting the observations in the ad libitum and diet-restricted groups, respectively. Multiple mice having the same concentration at the same death time are indicated by horizontally staggered symbols. The symbols also are staggered vertically to distinguish the 2 feeding protocols. The solid and dashed lines show the expected concentrations in the ad libitum and diet restricted groups, respectively, for reference mice (i.e., those with an initial body weight equal to the average).

Sex-Pluck Weight

Sex-pluck weights were available for all 84 mice without an NET and are plotted against time on study in Figure 4, along with reference curves that show the sex-pluck weights our model would predict for mice of an average initial body weight. We used a transformation of sex-pluck weight (i.e., the reciprocal of the square root) because it provided a better fit of the model to the data. Sex-pluck weight clearly

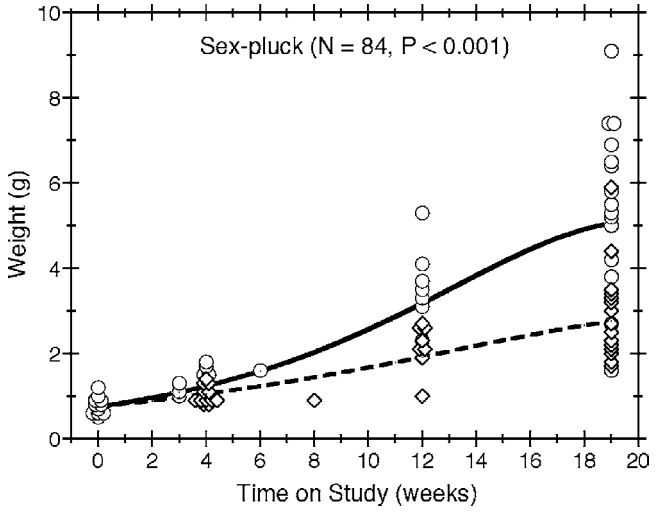

FIGURE 4.—Sex-pluck weight by time on study and feeding group. The combined weight of the prostate and accessory sex glands is plotted over time for all mice without an NET, with circles and diamonds depicting the observations in the ad libitum and diet-restricted groups, respectively. Multiple mice having the same weight at the same death time are indicated by horizontally staggered symbols. The symbols also are staggered vertically to distinguish the 2 feeding protocols. The solid and dashed lines show the expected weights in the ad libitum and diet-restricted groups, respectively, for reference mice (i.e., those with an initial body weight equal to the average).

increased over time, but compared to the mice fed ad libitum, the time trend was much reduced among diet restricted mice ($p < 0.001$).

Lobe-Specific Lesion Development and SV40 Immunostaining

Proliferative prostate lesions developed in a lobe specific manner. In the dorsal and anterior lobe, focal proliferations of hyperbasophilic, crowded epithelium developed in acini adjacent to normal epithelium (Figure 5A, 5B). SV40 immunostaining characteristics of these lobes showed positive staining of the lesional proliferative epithelium, but no staining of the normal epithelium (Figure 5C, 5D). In the anterior and lateral lobes, proliferative epithelial lesions were accompanied by thickening and proliferation of the adjacent smooth muscle wall of the acini (Figure 5E). This thickened acinar wall in the anterior prostate was immunopositive for SV40 (Figure 5F).

In the lateral and ventral lobes, lesions developed diffusely with epithelial cell crowding and hyperbasophilia distributed uniformly throughout all acini (Figure 5G, 5H). Likewise, SV40 staining was uniform throughout these lobes (Figure 5I, 5J).

With further lesion progression, the anterior and dorsal lobes showed distinct grade 5 intraluminal masses, which markedly expanded the acinus (Figure 5K). These lesions frequently became infarcted and presented as necrotic hemorrhagic masses (Figure 5L). Grade 6 lesions consisting effacement of acini with of sheets of poorly differentiated cells, proliferation of interstitial fibrous tissue and local invasion beyond the acinar wall (Figure 6A, 6B) were occasionally seen in the anterior and dorsal lobes also.

The lateral lobe frequently developed grade 5 lesions that were characterized by diffuse proliferation of the acinar epithelium that filled and expanded the acini, however distinct masses similar to those in the anterior and dorsal lobes were not observed. Occasionally focal grade 6 lesions characterized by proliferation of epithelium with less distinct acinar pattern were seen in the lateral lobe (Figure 6C). The ventral lobe had less lesion progression with time than the other lobes. Occasional focal grade 5 lesions appeared as solid proliferations of epithelium filling acinar lumens, but there was no expansion of acini. In some mice, the lateral lobe also had a prominent interstitial tissue proliferation between acini. This was not evident in the ventral lobe and was a useful histologic feature with which to distinguish the lateral lobe from the ventral lobe. The secretion within the acini generally had a lobe specific appearance earlier in development of proliferative lesions, being intensely eosinophilic and globular in the lateral lobe, and more basophilic and finely granular in the ventral lobe. This distinction, however, was lost in older animals, and the secretion was uniformly amphophilic and finely granular in the lateral and ventral lobes.

Neuroendocrine Tumors

NETs were observed in the ventral lobe of the prostate and in the urethra beneath the urothelium. NETs began as a proliferation of small basophilic cells within the acinar epithelium of the ventral lobe (Figure 6D), or in the submucosal glands of the urethra. As NETs developed in the ventral prostate they formed expansile masses, which first separated the epithelium from the basement membrane, then dissected and invaded through the basement membrane. NETs continued to expand within the interstitium (Figure 6E, 6F), separating and entrapping the acini and eventually obliterating the ventral lobe and when advanced, also the lateral lobes (Figure 6G). In the urethra, NETs developed in the submucosal glands outwardly compressing the skeletal muscle component surrounding the penis as well as causing intraluminal protrusion of the urothelium into the urethra (Figure 6H). Eventually the enlarging NET obstructed the urethral lumen (Figure 6I). Histologically, early NETs were composed of packets of cells separated by fine fibrous stroma and occasionally formed rosettes. Advanced NETs consisted of sheets of cells with marked cellular and nuclear pleomorphism and bizarre mitoses (Figure 6J). Sheets of viable neuroendocrine cells had zones of necrosis that surrounded islands of surviving cells with angiocentric orientation (Figure 6K).

NETs in the ventral prostate or urethra were present in a single mouse at 20 weeks and in a single mouse in both the ad libitum and diet restricted groups at the 24-week sacrifice. At 32 weeks, 2 mice in each of the ad libitum and diet restricted groups had NETs, with one of the ad libitum mice having NETs both in the ventral prostate and in the urethra. At the 39-week sacrifice, 5 mice in the ad libitum group and 2 in the diet restricted group had NETs. Of the 11 ad libitum mice dying prior to scheduled sacrifice, 7 had NETs and of the 5 diet-restricted mice that died early, 4 had NETs. Due to their size and location, NETs were considered by the evaluating pathologist to be the cause of death in 6 of the 7 ad libitum early death mice and in all 4 of the diet-restricted early death mice. Although there were more NETs in the ad libitum than the diet restricted groups both in mice surviving to scheduled sacrifice and in mice that died early, the

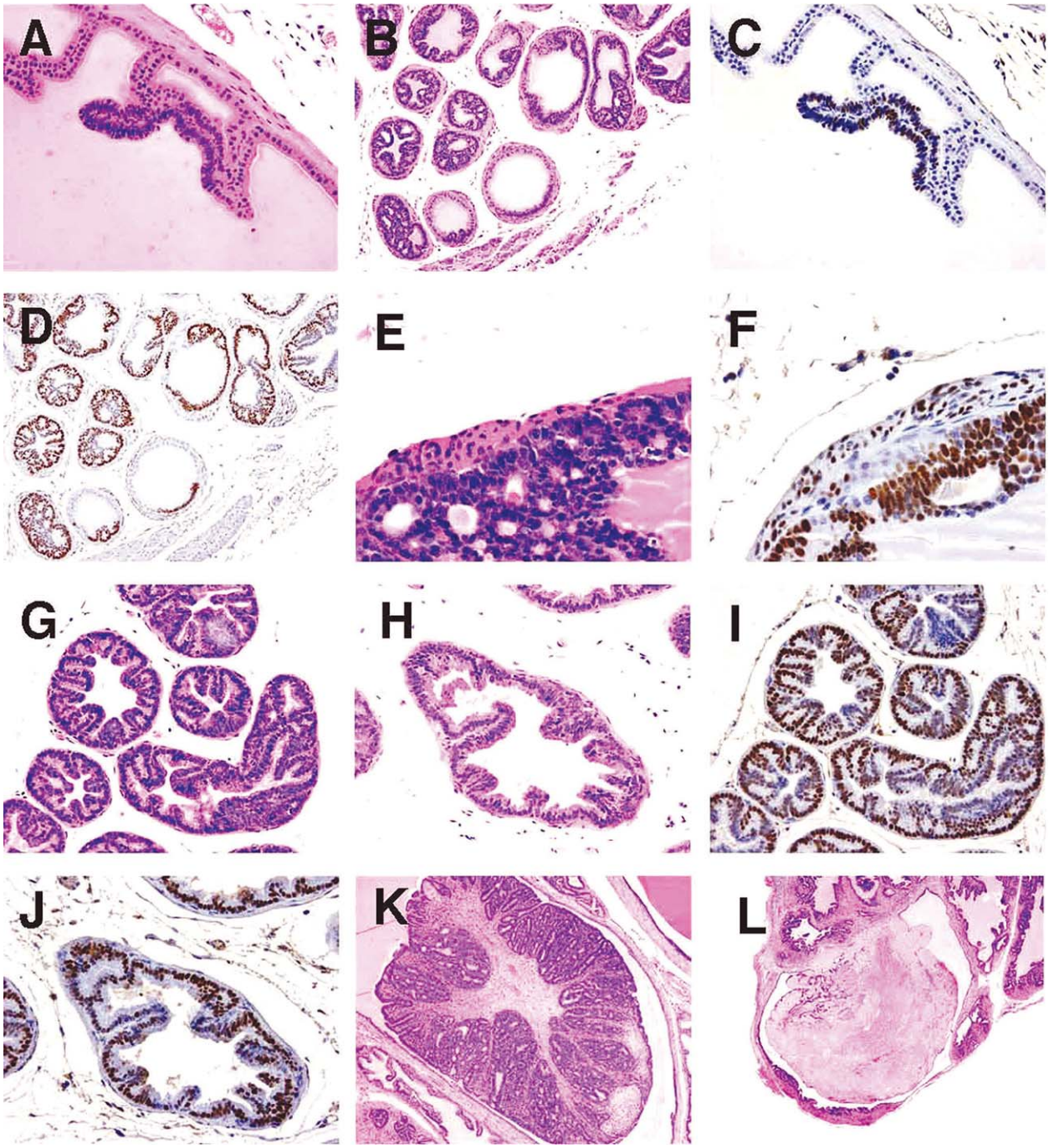

FIGURE 5.—(A) Anterior lobe. H&E. Region of focal epithelial hyperplasia; (B) Dorsal lobe. H&E. Focal areas of normal epithelium remaining in some acini; (C) Anterior lobe. SV40. Positively restricted to hyperplastic epithelium; (D) Dorsal lobe. SV40. Hyperplastic epithelium only shows positively; (E) Anterior lobe. H&E. Hyperplastic epithelium with adjacent proliferative smooth muscle wall; (F) Anterior lobe. SV40. Smooth muscle shows positively; (G) Lateral lobe. H&E. Epithelium lining acini is diffusely hyperplastic; (H) Ventral lobe. H&E. Epithelium lining acini is diffusely hyperplastic; (I) Lateral lobe. SV40. All epithelium shows positively; (J) Ventral lobe. SV40. All epithelium shows positively; (K) Anterior lobe in 39-week mouse. H&E. Grade 5 lesion expands lumen of acinus; and (L) Dorsal lobe in 32-week mouse. H&E. Infarcted grade 5 lesion expands acinus.

differences were not statistically significant. Neuroendocrine tumor metastases were seen in 12 of the 25 mice with NETs. There was distant metastasis to lymph nodes, kidneys, liver (Figure 6L), and lung, and local invasion to the striated muscle of the penis and the epididymis.

SV40 immunostaining was performed on NETs from 4 animals; one with NETs in the ventral prostate lobe, 2 with NETs in the urethra, and 1 with NETs in both locations. In all case, cells of the NETs had strong positivenuclear staining for SV40 (Figure 7A).

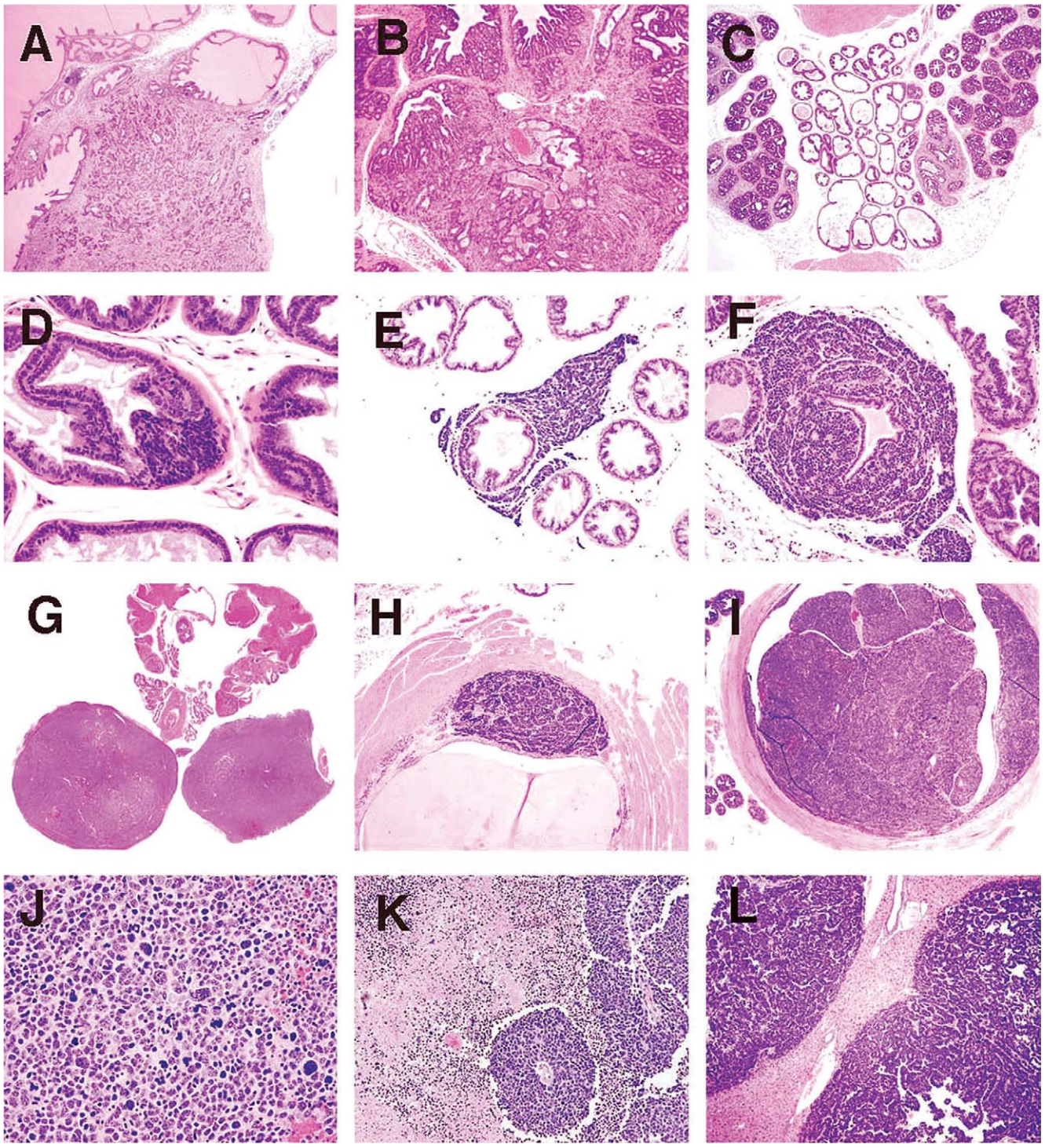

FIGURE 6.—(A) Anterior lobe in 32-week mouse. H&E. Grade 6 lesion showing local invasion; (B) Dorsal lobe in 39-week old mouse. H&E. Grade 6 lesion showing local invasion; (C) Lateral and ventral prostate lobes in 32-week old mouse. H&E. Prominent fibrous interstitial reaction is apparent in lateral lobes; (D) Ventral lobe. H&E. Neuroendocrine tumor arising in epithelium of acinus; (E) Ventral lobe. H&E. Neuroendocrine tumor between epithelium and basement membrane, with interstitial invasion; (F) Ventral lobe. H&E. Neuroendocrine tumor dissecting epithelial basement membrane and expanding into interstitial space; (G) Prostate and seminal vesicles. H&E. Neuroendocrine tumor obliterating ventral and lateral lobes; (H) Urethra. H&E. Neuroendocrine tumor arising beneath urothelium; (I) Urethra. H&E. Neuroendocrine tumor expanding and obstructing lumen; (J) Ventral lobe. H&E. Neuroendocrine tumor. Sheets of pleomorphic cells showing anisocytosis and anisokaryosis with bizarre mitoses; (K) Ventral lobe. H&E. Neuroendocrine tumor with areas of necrosis and angiocentric orientation of viable tumor cell focus; and (L) Liver. H&E. Neuroendocrine tumor metastases.

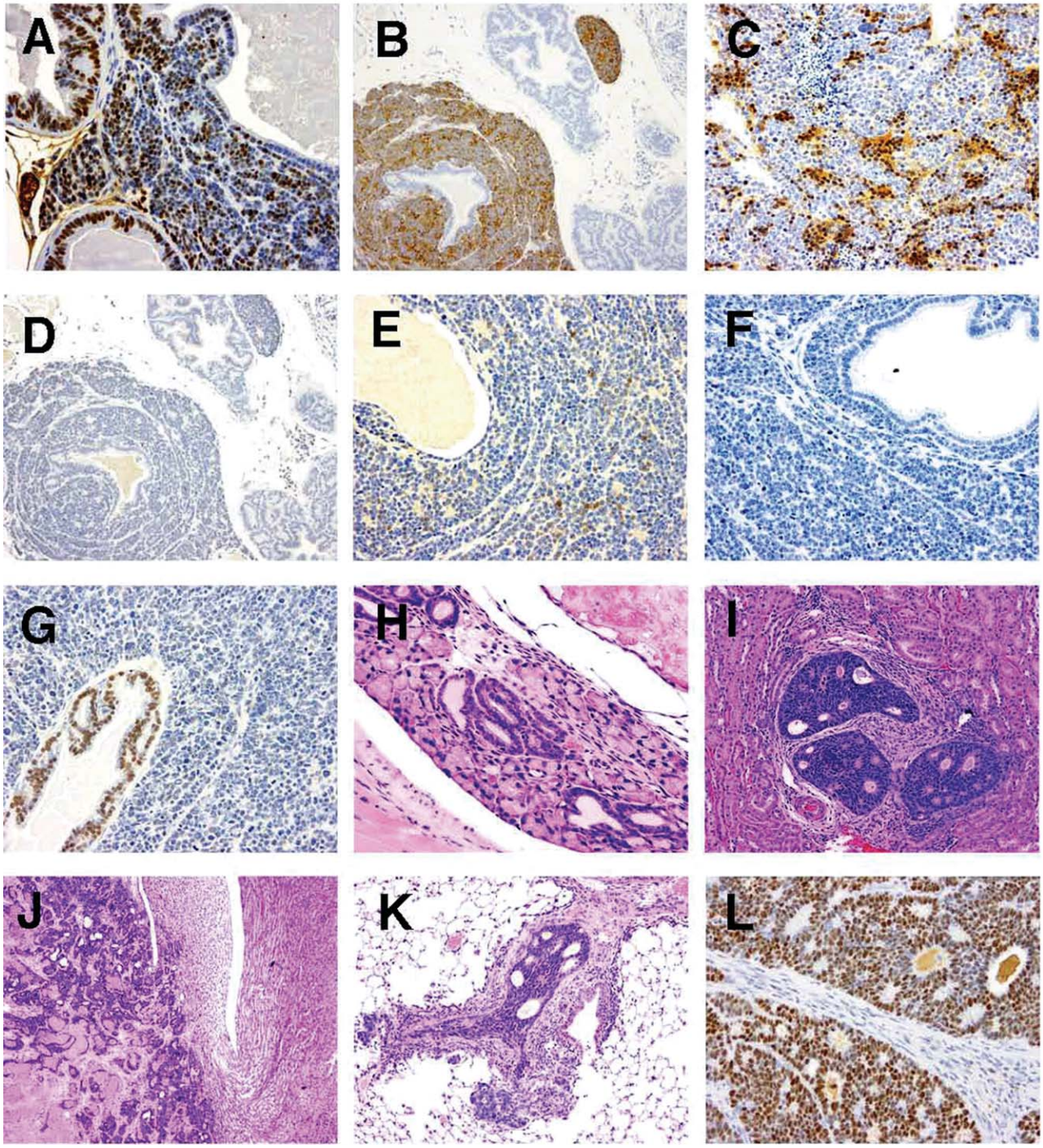

FIGURE 7.—(A) Ventral lobe. SV40. Positivity in prostatic epithelium and neuroendocrine cells; (B) Ventral lobe. Synaptophysin. Positivity in neuroendocrine cells. Prostatic epithelium negative; (C) Ventral lobe. NSE. Positivity in neuroendocrine cell aggregates; (D) Ventral lobe. Chromogranin A. Negative in neuroendocrine cells and prostatic epithelium; (E) Ventral lobe. Serotonin. Light positivity in neuroendocrine cell aggregates. Prostatic epithelium negative; (F) Ventral lobe. COX-2. Neuroendocrine cells and prostatic epithelium negative; (G) Ventral lobe. AR. Prostatic epithelium positive. Neuroendocrine tumor negative; (H) Submucosal glands of urethra. H&E. Foci of proliferative tubules; (I) Kidney. H&E. Tubulo-acinar tumor; (J) Kidney. H&E. Tubulo-acinar tumor effacing normal kidney architecture; (K) Lung. H&E. Tubulo-acinar kidney tumor metastasis; and (L) Kidney. SV40. Tubulo-acinar kidney tumor positive.

Neuroendocrine cell marker immunostaining was performed on NETs from 5 mice: 4 from ventral prostate, and 1 in both the ventral prostate and urethra. Results of this staining of NETs and the adjacent prostate epithelium are shown in Table 1; results of staining of all prostate lobes from an animal with advanced proliferative epithelial lesions, but not NETs, is also shown. All NETs stained for synaptophysin (Figure 7B), the intensity of which varied from moderately to markedly intense. Synaptophysin staining was sensitive and highly specific for neuroendocrine cells, and was

TABLE 1.—Immunostaining characteristics of neuroendocrine tumors and prostatic epithelium.

Mouse (age)	Tissue/lesion present	Synaptophysin	NSE	Chromogranin A	Serotonin	COX-2	AR
1 (32 wks)	Ventral lobe and urethra with NETs (early)	+++/0		0/0	+/+	0/0	+/++
2 (39 wks)	Ventral lobe with NET (early)	++/0	+/0		0/0	0	+
3 (31 wks)	Ventral lobe with NET (advanced)	++/0	++/0	0/0	+/0	0/0	+/++
4 (32 wks)	Ventral lobe with NET (advanced, with necrosis)	++/0	+++/0	0/0	+/0	0/0	+/+
5 (24 wks)	Ventral lobe with NET (advanced)	++/0	+++/0		+/0	0	
6 (39 wks)	Seminal vesicle, anterior and dorsal lobes	0	0		0	0	+
6 (39 wks)	Dorsal, lateral, and ventral lobes	0	0		0	0	

Five mice with prostate and NETs of various stages of development, and 1 mouse with prostate only were immunostained for synaptophysin, chromogranin A, NSE, serotonin, androgen receptor and cyclo-oxygenase-2. Intensity of staining is shown on 4 point scale.

NET staining/prostate epithelium staining. 0 = no staining; + = detectable staining; ++ = light staining; +++ = intense staining.

NET = neuroendocrine tumor.

NSE = neuron specific enolase. COX-2 = cyclo-oxygenase 2. AR = androgen receptor.

seen diffusely throughout the cytoplasm. In addition, intense synaptophysin staining was observed in the cytoplasm of neurons in the ganglia of the dorsal prostate and in scattered cells in the urethral urothelial and submucosal glands. Occasional staining of cytoplasmic granules in interstitial macrophages was also seen in negative controls, indicating this was nonspecific background.

NETs stained for NSE with high specificity and in most cases with high intensity. Staining occurred diffusely in the nucleus and cytoplasm with aggregates of positively stained cells interspersed (Figure 7C). Neuronal cells in adjacent ganglia showed strong staining for NSE, and served as a positive internal control. Prostatic epithelium did not stain for NSE. Chromogranin A immunostaining was not specific for NETs. Light granular staining was seen in both the nucleus and cytoplasm of both NETs and prostatic epithelium (Figure 7D). Serotonin was neither a sensitive nor a specific marker for NETs; tumors that stained strongly for synaptophysin and NSE did not stain, or had only light staining with serotonin (Figure 7E). Prostatic epithelium also on occasion stained for serotonin.

COX-2 staining was uniformly negative in both NETs and the prostate epithelium (Figure 7F). Urothelium that was present in profiles of the urethra on some tissue sections stained intensely for COX-2, and served as a positive internal control. Androgen receptor (AR) immunostaining showed very lightly stained NETs, but stained all prostate epithelium (Figure 7G).

Suburethral Glands

In aging TRAMP mice, the suburethral glands frequently contained proliferations of tubules lined by a single layer of basophilic epithelial cells (Figure 7H). These structures did not appear to progress to large space occupying tumors nor differentiated neuroendocrine tumors. They exhibited positivite immunostaining for SV40, but did not stain for neuroendocrine markers, AR and Cox-2.

Tubulo-Acinar Kidney Tumors

Distinctive renal tumors were observed in an ad libitum mouse and a diet restricted mouse from the 39-week sacrifice groups. These tumors consisted of poorly differentiated tubular and acinar formations lined by a multilayered epithelium composed of small basophilic cells (Figure 7I). These structures had a central lumen containing necrotic cell debris. The lining epithelium showed a cribriform pattern characterized by numerous small lumens within the epithelium that were either empty or contained amorphous eosinophilic material. These tumors effaced the kidney architecture with a zone of expansion into the viable kidney parenchyma. There were extensive areas of necrosis away from this zone of expansion (Figure 7J). Metastases were observed in the lymph nodes, liver, pancreas, and lung (Figure 7K). Tubulo-acinar kidney tumors had positive immunostaining for SV40 (Figure 7L), but were negative for synaptophysin, NSE, serotonin, AR, and Cox-2. They exhibited light, stippled, predominantly nuclear, immunostaining for chromogranin A, similar to that of the NETs and prostatic epithelium.

DISCUSSION

We have shown that dietary restriction, applied to TRAMP mice with advanced prostate neoplasia, is effective in retarding the progression of tumors. As shown in our earlier work, diet restriction initiated at 7 weeks (Suttie et al., 2003), the approximate age of onset of puberty in these mice, reduced the progression of proliferative lesions at 11 and 20 weeks of age. This suggests that diet restriction in the TRAMP model is useful in the study of the initiation and early development of prostate tumors. Results reported in this paper suggest that the processes that play a role in early lesion development and that can be ameliorated by dietary restriction from puberty, still appear to be active in the established tumors. In humans it has been demonstrated that obesity is associated with higher-grade prostate cancers and higher recurrence rates following radical prostatectomy (Amling et al., 2003). Therefore, our observations with established lesions suggest that the TRAMP mouse may also be a clinically relevant model to study the mechanisms by which dietary restriction provides this clinical advantage to prostate cancer patients following diagnosis, both alone and in combination with other surgical and medical therapies.

We previously noted that in the TRAMP mouse prostate, proliferative lesions develop in a lobe-specific manner (Suttie et al., 2003). In the anterior and dorsal lobes, lesions appear initially as focal proliferations of hyperbasophilic epithelium. In contrast, in the lateral and ventral lobes, lesions develop diffusely involving the epithelium throughout all acini, which becomes diffusely hyperbasophilic with cell crowding. In the anterior and dorsal lobes, lesions progress to expand acini and form distinct intraluminal masses which, with advancing age seen in the present study sometimes become infarcted and necrotic. In both our earlier studies and the present study we observed tumor invasion beyond the acinar wall into the adjacent stroma almost exclusively in the anterior and dorsal

lobes. These grade 6 lesions present as sheets of poorly differentiated acini with a prominent interstitial fibrous reaction. Lateral and ventral lobes develop grade 5 lesions, and occasionally in the lateral lobe, grade 6 lesions, without distinct intraluminal masses.

We performed SV40 staining as an indicator of probasin gene activity on early lesions in these lobes. The SV40 staining characteristics are also lobe specific and show a distribution similar to the histological appearance of lesion development, i.e., focally within adjacent unstained normal epithelium in the anterior and dorsal, and diffusely in the lateral and ventral lobes. These SV40 staining characteristics of the prostate indicates probasin gene activity only in proliferating epithelium, not in the normal tissues, and that this activity is lobe specific.

Proliferation of the smooth muscle component of the wall of the anterior and dorsal lobes is also a feature of TRAMP prostate lesion development. Interactions between the prostatic epithelium, and fibroblasts and smooth muscle cells of the associated stroma have been identified as important in prostatic organogenesis and carcinogenesis (Cuhna et al., 2002; Nyska et al., 2002). The positive SV40 immunoreactivity in the proliferative smooth muscle wall of the anterior and dorsal lobes in the TRAMP mouse indicates that this proliferation is a probasin driven process, and not simply secondary to the growth of the neoplastic epithelial component. It is therefore probable that the stroma is actively involved in the development of neoplasms in these lobes. We previously observed herniation of epithelium within this proliferating stroma (Suttie et al., 2003) and interpreted this as a process primarily due to entrapment within proliferating stroma. The finding of SV40 staining within the proliferating stroma suggests it may instead be an important aspect in development of malignancy in the anterior and dorsal lobes.

In the lateral lobe of some animals, higher-grade epithelial lesions were accompanied by an increase in interstitial tissue between acini. Unlike the anterior and dorsal lobes, this fibrous component appeared sporadically, and there was no obvious correlation with the grade of lesion within the acini and did not stain for SV40. This histological feature may be a useful characteristic by which to distinguish the lateral and ventral lobes in these animals, since lobe specific features of epithelial cell morphology and secretion are not present in the more advanced lesions. In likelihood, it represents a stromal reaction to the epithelial lesions and is not involved in the pathogenesis.

The insulin-like growth factor axis system is composed of 2 mitogenic ligands (IGF-1 and IGF-II), 2 receptors (IGF-1R and -2R), and 6 binding proteins (IGFBP-1 to IGFBP-6). IGFBPs function through regulation of IGF bioavailability for IGF receptors (Moore et al., 2003). The IGF axis is a key endocrine, autocrine, and paracrine signaling system, modulating cell proliferation, apoptosis, and tumorigenesis (Dunn et al., 1997) and is involved in progression of cancers of the prostate, breast, urinary bladder, and lung (Kari et al., 1999; Grimberg and Cohen, 2000). Prostate-specific antigen (PSA), which is expressed by prostate cancers and elevated levels are associated with prostate carcinoma and benign prostatic hyperplasia (Karr et al., 1995). PSA cleaves IGFBP-3, releasing IGF-1 (Cohen et al., 1992). The IGF axis mediates the anticarcinogenic effect of dietary retriction (Kari et al., 1999) with serum IGF-1 being lowered in humans and rodents subjected to a dietary restriction regimen. In-vitro studies have shown reduced growth and increased apoptosis/necrosis of prostatic cells cultured in serum that contained reduced levels of IGF-1 obtained from individuals given a reduced fat diet and also exercise (Ngo et al., 2002). In mice with chemically induced cancer of the urinary bladder, diet-restriction-delayed tumor progression, IGF-1 supplementation administered via osmotic minipumps, increased cancer progression in dietary-restricted mice independently of bodyweight (Dunn et al., 1997). We have also seen this effect in the TRAMP mouse prostate. Diet restricted mice supplemented with IGF-1 increased prostate tumor grades similar to those seen in ad libitum fed mice (unpublished data).

In the present study, the reduction in serum IGF-1 levels seen with dietary restriction did not show statistical significance. Therefore, the link between the effect of dietary restriction on reduction in tumor grade in the dorsal and lateral lobe and effects on serum IGF-1 levels could not be confirmed.

Our earlier work with diet-restriction initiated at 7 weeks (puberty) demonstrated that by 20 weeks, there was a reduction in lesion progression in the anterior, dorsal and lateral lobes, but not in the ventral lobe. In the present study, similar effects occurred in the dorsal, and lateral lobes. There was little difference in mean lesion grade in the ventral lobe between 20 and 39 weeks, and no difference with diet-restriction. Furthermore, there were no malignant epithelial lesions in the ventral lobe. This suggests that there is a point beyond which ventral lobe lesions do not progress. However, the ventral lobe was the source of prostatic neuroendocrine tumors, which were identified as a significant cause of mortality in most of the early deaths of our TRAMP mice.

Neuroendocrine cells comprise a small percentage of the prostatic epithelial cells scattered among the acinar and ductular epithelial cells where they secrete a variety of growth factors (Garabedian et al., 1998). Neuroendocrine tumors are reported in human prostate cancers (Chuang et al., 2003) and in probasin driven mouse models of prostate cancer (Garabedian et al., 1998; Masumori et al., 2001), including the TRAMP (Kaplan-Leftko et al., 2003). In TRAMP mice, NETs are considered a subset of poorly differentiated carcinomas (Martiniello-Wilks et al., 2003), which undergo an epithelial to neuroendocrine shift as a stochastic event (Kaplan-Leftko et al., 2003). We observe NETs developing only in the ventral lobe of the prostate. We have not observed NETs developing from higher grade tumors in either the ventral or other prostatic lobes. Similar to the development of NETs in FVB/N mice containing the SV40 T-Ag (Garabedian et al., 1998), the NETs in our study developed in the prostate as proliferations of cells located between the basement membrane and overlying layer of epithelial cells. However, unlike NETs in FVB/N mice, in the present study, NETs did not develop in the acinar lumen as tufts, but dissected the basement membrane and proliferated in the interstitium, eventually effacing the normal architecture of the ventral and the lateral lobes and entrapping acini of both lobes. In the urethra, NETs also developed beneath the urothelium, possibly in the epithelium of the urethral glands.

The NETs were considered to be the cause of death in the majority of early death animals. In some cases they obliterated the prostate acini, initially in the ventral lobe, and

subsequently the lateral lobes. We have analyzed epithelial tumors in the prostate lobes only among mice without NETs since we considered the NETs distinct tumor types that do not develop through the same continuum of lesion progression observed with the epithelial neoplasms. Some researchers have utilized grading schemes that do not consider lesion development as a continuum, but instead as a series of distinct lesion types (Shibata et al., 1996; Masumori et al., 2001).

They also consider NETs as a poorly differentiated carcinoma with neuroendothelial differentiation. Since our grading scheme was designed to yield a single numerical score for lesion development in each lobe, thereby allowing easy comparison across relatively large numbers of animals, we did not consider it appropriate to include neuroendocrine pattern tumors in this grading scheme. Furthermore, since the presence of advanced NETs was associated with morbidity that may have significantly affected dietary intake with consequently, unpredictable effects on the development of the epithelial tumors in the prostate, we considered it appropriate to exclude all mice with a diagnosis of NET from the final analysis of epithelial tumor grade in the prostate. Unlike other researchers, we did not observe metastases from epithelial tumors in our mice. However, we frequently observed metastases in mice with NETs. Two neuroendocrine markers, synaptophysin and chromogranin A, are reported to stain neuroendocrine cells in SV40 T-Ag-positive NETs (Garabedian et al., 1998). Kaplan-Leftko et al. (2003) have used synaptophysin to identify NETs in TRAMP mice. In our panel of neuroendocrine markers we also included NSE and serotonin, which are used for diagnosis of NETs in other species, including humans (Bostwik et al., 2002). Synaptophysin and NSE were both sensitive and specific markers for NETs with no staining of adjacent prostatic acini. Serotonin was less sensitive than synaptophysin and was not specific, with the prostatic epithelium also staining. Chromongranin A did not stain the NETs. Synaptophysin and NSE are therefore considered to be valuable in the identification of neuroendocrine tumors in TRAMP mice. The presence of neurones in the ganglia adjacent to the anterior prostatic lobe provides highly specific and sensitive internal positive controls for these immunostains.

Human NETs do not express androgen receptors (Garabedian et al., 1998) and are reported to be a hormone refractory prostate cancer in men. Kaplan-Leftko et al. (2003) reported variable AR immunostaining in some "poorly differentiated" tumors that they considered had developed neuroendocrine features rather than arising specifically from neuroendocrine precursors. The NETs in our TRAMP mice did not show significant staining for AR, and did appear to arise specifically from neuroendocrine precursors thereby suggesting a similarity with the human NETs. This would suggest that some aged TRAMP mice with high incidence of NETs may be a valuable model for the study of hormone refractory prostate cancer.

COX-2 is overexpressed in human prostate cancers and, in human epidemiological studies COX-2 inhibitors are reported to reduce the risk of prostate cancer (Gupta et al., 2004). Therefore, some researchers have used nonsteroidal anti-inflammatory drugs to inhibit prostate cancer progression in the TRAMP mouse (Wechter et al., 2000; Gupta et al., 2004). In these experiments, prostate tumors expressed COX-2 and associated mRNA, although expression of the enzyme may be down-regulated in advanced lesions. In our TRAMP mice, we were unable to demonstrate COX-2 in either NETs or other proliferative prostate lesions. The presence of strong, specific COX-2 immunostaining of transitional epithelium in profiles of ureter in the sections, suggests this immunostain was a functional marker. The absence of immunoreactivity for COX-2 in the prostate of our mice is unexplainable, but, it may reflect variation in expression of COX-2 in certain TRAMP mice.

The tubulo-acinar tumors we have observed occasionally in the kidney of TRAMP mice (including in one female from our breeding colony) had positive SV40 immunostaining, suggesting that they may be probasin driven. The absence of staining with neuroendocrine markers, however, indicates they are either not of neuroendocrine origin or are poorly differentiated. Neuroblastomas arising in the tongue of the transgenic rats with probasin-driven SV40 large T antigen (Asamoto et al., 2001) are morphologically similar to the kidney tumor in TRAMP mice and were immunoreactive for synaptophysin. Human neuroblastomas are also reported to be positive for NSE, and Chromogranin A and synaptophysin (Belchis, 2002). In the present study, the kidney tumors did not have positive immunostaining for any of these markers. We propose that this tumor may have a primitive origin, possibly from remnants of embryonic kidney or other embryonic ductular structures in this region.

In conclusion, this work demonstrated that, similar to dietary restriction introduced at puberty, dietary restriction does retard epithelial lesion development later in lesion development. Also, NETs are an important factor influencing mouse survival in the TRAMP mouse.

ACKNOWLEDGMENTS

This work was supported by NIEHS [N01-ES-95434, N01-ES-95446]. We gratefully acknowledge Dr. N. Greenberg of the Fred Hutchinson Cancer Research Center, Seattle, Washington, for supplying the mice to establish our TRAMP colony. We thank Julie Foley of NIEHS for SV40 immunostaining, Dr. Gordon Hard of Tairua, New Zealand for expert opinion on the tubulo-acinar tumors in the kidney and the Toxicology, Histology, and Animal Care staff of ILS for their expertise and dedication in running the animal studies and producing the pathological specimens.

REFERENCES

Amling, C. L., Riggenburgh, R. H., Sun, L., Moul, J. W., Lance, R. S., Kusuda, L., Sexton, W. J., Soderdahl, D. W., Donahue, T. F., Foley, J. P., Chung, A. K., and McLeod, D. G. (2004). Pathologic variables and recurrence rates as related to obesity and race in men with prostate cancer undergoing radical prostatectomy. *J Clin Oncol* **1;22**(3), 439–45.

Asamoto, M., Hokaiwado, N., Cho, Y. M., Ikeda, Y., Takahashi, S., and Shirai, T. (2001). Metastasizing neuroblastomas from taste buds in rats transgenic for the Simian virus 40 large T antigen under control of the probasin gene promoter. *Toxicol Pathol* **29**(3), 363–8.

Belchis, D. (2002). Diagnostic immunohistochemistry of pediatric small round cell tumors. In Diagnostic Immunohistochemistry. Dabbs DJ. Churchill Livingstone, Philadelphia. pp. 517–35.

Bostwick, D. G., Qian, J., and Ramnani, D. M. (2002). Immunohistochemistry of the prostate and bladder, testis, and renal tumors. In Diagnostic Immunohistochemistry. (DJ Dabbs, ed.), pp. 407–85. Churchill Livingstone, Philadelphia.

Chuang, C. K., Wu, T. L., Tsao, K. C., and Liao, S. K. (2003). Elevated serum chromogranin A precedes prostate-specific antigen elevation and predicts failure of androgen deprivation therapy in patients with advanced prostate cancer. *J. Formos. Med Assoc* **102**(7), 480–5.

Cohen, P., Graves, H. C., and Peehl, D. M. et al. (1992). Prostate-specific antigen (PSA) is an insulin-like growth factor binding protein-3 protease found in seminal plasma. *J Clin Endocrinol Metab* **75**, 1046–53.

Cunha, G. R., Hayward, S. W., and Wang, Y. Z. (2002). Role of stroma in carcinogenesis of the prostate. *Differentiation* **70**(9–10), 473–85.

Demark-Wahnefried, W., Price, D. T., Polascik, T. J., Robertson, C. N., Anderson, E. E., Paulson, D. F., Walther, P. J., Gannon, M., and Vollmer, R. T. (2001). Pilot study of dietary fat restriction and flaxseed supplementation in men with prostate cancer before surgery: exploring the effects on hormonal levels, prostate-specific antigen, and histopathologic features. *Urology* **58**(1), 47–52.

Dunn, S. E., Hardman, R. A., Kari, F. W., and Barrett, J. C. (1997). Insulin-like growth factor 1 (IGF-1) alters drug sensitivity of HBL100 human breast cancer cells by inhibition of apoptosis induced by diverse anticancer drugs. *Cancer Res* **57**, 2687–93.

Foster, B. A., Giingrich, J. R., Kwon, E. D., Madias, C., and Greenberg, N. M. (1997). Characterization of prostatic epithelial cell lines derived from transgenic adenocarcinoma of the mouse prostate (TRAMP) model. *Cancer Res* **57**, 3325–30.

Garabedian, E. M., Humphrey, P. A., and Gordon, J. I. (1998). A transgenic mouse model of metastatic prostate cancer origination from neuroendocrine cells. *Proc Natl Acad Sci* **95**, 15382–7.

Gingrich, J. R., Barrios, R. J., Morton, R. A., Boyce, B. F., DeMayo, F. J., Finegold, M. J., Angelopoulou, R., Rosen, J. M., and Greenburg, N. M. (1994). Metastatic prostate cancer in a transgenic mouse. *Cancer Res* **56**, 4096–102.

Giovannucci, E. (1995). Epidemiologic characteristics of prostate cancer. *Cancer* **75**, 1766–77.

Greenberg, N. M., DeMayo, F., Finegold, M. J., Medina, D., Tilley, W. D., Aspinall, J. O., Cunha, G. R., Donjacour, A. A., Matusik R. J., and Rosen, J. M. (1995). Prostate cancer in a transgenic mouse. *Proc Natl Acad Sci USA* **92**, 3439–43.

Greenberg, N. M., DeMayo, F. J., Sheppard, P. C., Barrios, R., Lebovitz, R., Finegold, M., Angelopoulou, R., Dodd, J. G., Duckworth, M. L., Rosen, J. M., and Matusik, R. J. (1994). The rat probasin gene promoter directs hormonally and developmentally regulated expresion of a heterologous gene specifically to the prostate in transgenic mice. *Mol Endocrinol* **8**, 230–9.

Grimberg, A. and Cohen, P. (2000). Role of insulin-like growth factors and their binding proteins in growth control and carcinogenesis. *J Cell Physiol* **183**, 1–9.

Gupta, S., Hastak, K., Ahmad, N., Lewin, J. S., and Mukhtar, H. (2001). Inhibition of prostate carcinogenesis in TRAMP mice by oral infustion of green tea polyphenols. *Proc natl Acad Sci* **98**(18), 10350–5.

Hubert, M.-F., Laroque, P., Gillet, J.-P., and Keenan, K. P. (2000). The effects of diet, *ad libitum* feeding, and moderate and severe dietary restriction on body weight, survival, clinical pathology parameters, and cause of death in control Sprague–Dawley rats. *Toxicol Sci* **58**, 195–207.

Jemal, A., Thomas, A., Murray, T., and Thun, M. (2002). Cancer statistics, 2002. *CA Cancer J Clin* **52**, 23–47.

Kaplan, E. L., and Meier, P. (1958). Nonparametric estimation from incomplete observations. *J Amer Stat Assoc* **53**, 457–81.

Kaplan-Leftko, P. J., Chen, T.-M., Ittmann, M. M., Barrios, R. J., Ayala, G. E., Huss, W. J., Maddison, L. A., Foster, B. A., and Greenburg, N. M. (2003). Pathology biology of autochthonous prostate cancer in a pre-clinical transgenic mouse model. *The Prostate* **55**, 219–37.

Kari, F. W., Dunn S. E., and French, J. E. (1999). Roles for insulin-like growth factor-1 in mediating the anti-carcinogenic effects of caloric restriction. *J Nutr Health Aging* **3**, 92–101.

Karr, J. F., Kantor, J. A., and Hand, P. H. (1995). The presence of prostate-specific antigen-related genes in primates and the expression of recombinant human prostate-specific antigen in a transfected murine cell line. *Cancer Res* **55**, 2455–62.

Lee, M. M., Gomez, S. L., Chang, J. S., Wey, M., Wang, R.-T., and Hsing A. W. (2003). Soy and isoflavone consumption in relation to prostate cancer risk in China. *Cancer Epidemiol, Biomarkers Prevention* **12**, 665–8.

Martiniello-Wilks, R., Dane, A., Mortensen, E., Jeyakumar, G., Wang., X. Y., and Russell, P. J. (2003). Application of the transgenic adenocarcinoma mouse prostate (TRAMP) model for pre-clinical therapeutic studies. *Anticancer Res* **23**, 2633–42.

Masumori, N., Thomas, T. Z., Chaurand, P., Case, T., Paul, M., Kasper, S., Capriolo, R. M., Tsukamoto, T., Shappell, S. B., and Matusik, R. J. (2001). A Probasin-Large T antigen transgenic mouse line develops prostate adenocarcinoma and neuroendocrine carcinoma with metastatic potential. *Cancer Res* **61**, 2239–49.

Moore, M. G., Wetterau, L. A., and Francis, M. J. (2003). Novel stimulatory role for insulin-like growth factor binding protein-2 in prostate cancer cells. *Int J Cancer* **105**, 14–19.

Neter, J., Wasserman W., and Kutner, M. (1985). Applied Linear Statistical Models, 2nd Edition. Richard D. Irwin Inc., Homewood, IL.

Ngo, T. H., Barnard, R. J., Cohen, P., Freedland, S., Tran, C., deGregorio, F., Elshimali, Y. I., Herber, D., and Aronson, W. J. (2003). Effect of isocaloric low-fat diet on human LAPC-4 prostate cancer xenografts in severe combined immunodeficient mice and the insulin-like growth factor axis. *Clin Cancer Res* **9**(7), 2734–43.

Nyska, A., Dayan, A., and Maronpot, R. R. (2002). New tools in therapeutic research–prostatic cancer and models. *Toxicologic Pathology* **30**(2), 283–7.

Nyska, A., Suttie, A., Lomnitski, L., Bakshi, S., Grossman, S., Bergman, M., Ben-Shaul, V., Crocket, P., Haseman, J. K., Moser, G., Goldsworthy, T., and Maronpot, R. R. (2003). Slowing tumorigenic progression in tramp mice and prostatic carcinoma cell lines using natural antioxidant from spinach, NAO—a comparative study of three antioxidants *Toxicol Pathol* **31**, 39–51.

Pugh, T. D., Oberley, T. D., and Weindruch, R. (1999). Dietary intervention at middle age: caloric restriction but no dehydroepiandrosterone sulfate increases lifespan and lifetime cancer incidence in mice. *Cancer Research* **59**, 1642–8.

Raghow, S., Kuliyev, E., Steakley, M., Greenberg, N., and Steiner, M. S. (2000). Efficacious chemoprevention of primary prostate cancer by flutamide in an autochthonous transgenic model. *Cancer Res* **60**, 4093–7.

Shibata, M. A., Ward, J. M., Devor, D. E., Liu, M. L., and Green, J. E. (1996). Progression of prostatic intraepithelial neoplasia to invasive carcinoma in C3(1)/SV40 large T antigen transgenic mice: histopathological and molecular biological alterations. *Cancer Res* **56**, 4894–903.

Suttie, A., Nyska, A., Haseman, J. K., Moser, G. J., Hackett, T. R., Goldsworthy, T. L., and Maronpot, R. R. (2003). A grading scheme for the assessment of proliferative lesions in the mouse postate in the TRAMP Model. *Toxicol Pathol.* **31**, 31–38.

Suwa, T., Nyska, A., Haseman, J. K., Mahler, J. F., and Maronpot, R. R. (2002). Spontaneous lesions in control B6C3F_1 mice and recommended sectioning of male accessory sex organs. *Toxicol Pathol* **30**, 228–34.

U.S. Department of Health and Human Services (1996). *Guide for the Care and Use of Laboratory Animals.* National Academy Press, Washington, DC.

Wechter, W. J., Leipold, D. D., Murray, E. D., Jr., Quiggle, D., McCracken, J. D., Barrios, R. S., and Greenberg, N. M. (2000). E-7869 (*R*-Flurbiprofen) Inhibits Progression of Prostate Cancer in theTRAMP mouse. *Cancer Res* **60**, 2203–8.